ISBN: 978-3-95450-236-3 ISSN: 2673-5350 doi:10.18429/JACoW-IBIC2023-TUP005

COMMISSIONING THE BEAM-LOSS MONITORING SYSTEM OF THE LCLS SUPERCONDUCTING LINAC*

Alan S. Fisher†, Namrata Balakrishnan, Garth Brown, Edward Chin, William G. Cobau, John E. Dusatko, Bryce T. Jacobson, Sung Kwon, Jeremy Mock, Jino Park, Jeremy Pigula, Evan Rodriguez, Jacob Rudolph, Daniel Sanchez, Leonid Sapozhnikov, James J. Welch
SLAC National Accelerator Laboratory, Menlo Park, California, USA

Abstract

A 4-GeV superconducting linac has been added to the LCLS x-ray FEL facility at SLAC. Its 120-kW, 1-MHz beam requires new beam-loss monitors (BLMs) for radiation protection, machine protection, and diagnostics. Long radiation-hard optical fibres span the full 4 km from the electron gun of the SC linac to the final beam dump. Diamond detectors at anticipated loss points and other points of concern provide local protection. Detector signals are continuously integrated with a 500-ms time constant and compared to a loss threshold. If crossed, the beam is halted within 0.1 ms. Commissioning began in March 2022 with the 100-MeV injector and with RF processing of the cryomodules. At IBIC 2022 last September, we presented commissioning results from the injector BLMs. In October, the beam accelerated through the full linac, passed through the bypass transport line above the LCLS copper linac, and stopped at an intermediate dump. In August it continued through the soft x-ray undulator and achieved first lasing. Here we present BLM commissioning at energies up to 4 GeV and rates up to 100 kHz. We discuss measurements and software using the fast diagnostic-waveform output to localize beam losses and to detect wire-scanner signals.

INTRODUCTION

Over the past few years, SLAC removed the first km of the 3-km copper normal-conducting (NC) copper linac and replaced it with a superconducting (SC) linac with 35 12-m-long cryomodules operating at f_{RF} = 1.3 GHz and two third-harmonic cryomodules. Each has 8 RF cavities and operates at a temperature of 2°K. All have been installed in the first 700 m of the tunnel. The SC linac, driven with continuous-wave (CW) RF power, produces 4-GeV bunches with variable spacing at rates up to 1 MHz (f_{RF}/1400). The 750-keV electron gun is also driven by CW RF, but at 186 MHz (f_{RF}/7) and followed by a 1.3-GHz buncher. A planned high-energy (HE) upgrade in the remaining 300 m will later double the energy. Before this doubling, the beam power at full rate and at a maximum bunch charge of 300 pC will reach 120 kW. At this time, the full linac has been commissioned to 3.5 GeV and first lasing has been achieved in the soft x-ray (SXR) undulator at 1 kHz.

The risk of damaging beam loss led to the development of a new protection system, including long optical fibres (long beam-loss monitors, LBLMs) that cover the full 4 km from gun to dump in sections of up to 200 m, and diamond detectors (point beam-loss monitors, PBLMs) that protect small sections or devices such as collimators [1].

At the previous IBIC, in September 2022, only the injector region, the first 50 m through the first cryomodule (80 to 100 MeV), had been commissioned. We reported then [2] on the initial performance of the LBLMs and the one PBLM in this low-energy region. Over the past year, the full beam-loss system has been tested. We now can provide a more complete look at its performance.

LONG BEAM-LOSS MONITORS

Integrated Beam-Loss Signals

Radiation-hard quartz optical fibres (FBP600660710 from Polymicro) run parallel to the beam (z direction, west to east), in lengths of up to 200 m. Beam losses generate showers that pass through the beampipe and fibre, emitting Cherenkov light that travels to the ends of the fibre. At the downstream end, the light is measured by a photomultiplier tube (PMT) outside the tunnel, in a rack-mounted chassis.

The beam can pulse at a steady 1 Hz to 1 MHz, in single shots, or with variable spacings. Consequently, protection is based not on shot-by-shot loss but from the total loss in 500 ms, integrated by an *RC* circuit. This signal is amplified and compared on the board to the Beam Containment System (BCS) threshold. BCS can stop the beam, the RF cavities and, if necessary, the electron gun. It is analogue, simple, and robust, without awareness of beam rate or the beamline causing the loss. The same integrated signal is buffered and sent to the Machine Protection System (MPS) [3], where it is digitised and compared to a second level below the BCS threshold, to trip the beam first. It is aware of timing and beamline selection. It acts by blocking the photocathode laser or by halting downstream kickers that direct the beam. If dark current causes persistent losses, MPS escalates to BCS, which can halt the gun RF.

The SC linac regions L0B through L3B (here "B" distinguishes these from the LCLS NC linac, in the third km) are separated by warm regions for collimation and bunch compression. Each region is spanned by two fibres, linked for redundant protection in two BCS "chains", also called "A" and "B". Linac A-chain fibres are on the north wall at beam height and 90 cm horizontally from the beam. B fibres are on the ceiling and to the south, at a 3-m distance. The different views give the pair similar but not identical responses. Because the thick cryomodule walls require extra gain, fibres span warm or cold regions, but not both. PMT gains for B fibres are somewhat higher to compensate for greater distance. Fibre mounting in transport lines is different; some have only an A fibre.

* SLAC is supported by the U.S. Department of Energy, Office of Science, under contract DE-AC02-76SF00515.
† afisher@slac.stanford.edu

ISBN: 978-3-95450-236-3 ISSN: 2673-5350 doi:10.18429/JACoW-IBIC2023-TUP005

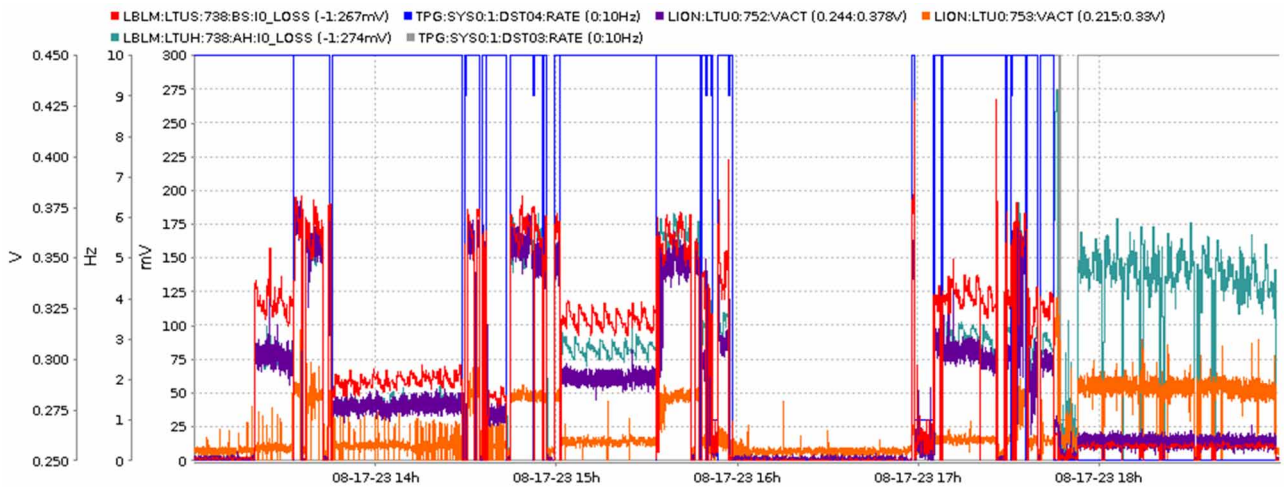

Figure 1: Comparison of LBLM and LION signals in the LTU as 10-Hz beam was switched from the soft x-ray (SXR, north side) beamline to the hard x-ray (HXR, south) line. Blue: Rate to SXR. Grey: Rate to HXR. Red: LBLM on SXR side. Green: LBLM on HXR side. Purple: LION on SXR side. Orange: LION on HXR side. Both LBLMs and LIONs responded to the switch and gave similar signals, but the LIONs appear noisier.

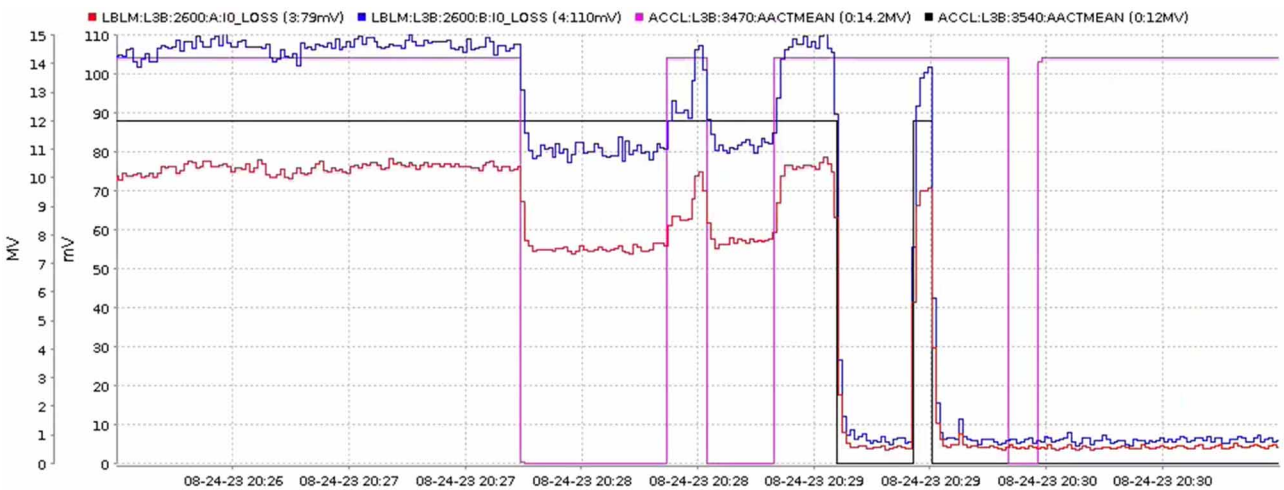

Figure 2: LBLM signals from cryomodule field emission. Two fibres span the downstream half of L3B, on the wall (red) and ceiling (blue). Both signals suddenly jumped up, and MPS tripped the photocurrent. The gun dark current was low. Cryomodules along this region were cycled off and on, one at a time. Losses dropped somewhat with module 34 cavity 7 (CM34-7, magenta) but went nearly to zero when CM35-4 (black) was shut off.

Previously long coaxial ionization chambers (LIONs) protected regions of NC beamlines. Modelling showed that these are not suited to the SC beam: at high loss rates the space charge of slowly moving ions can screen the internal bias field, suppressing the response [1]. Figure 1 compares two fibres and two LIONS in the linac-to-undulator (LTU) transport tunnel. It shows one of each type near the beamline leading to the hard x-ray undulator (south side of the tunnel) and another pair near the soft x-ray (north) side. As a 10-Hz beam was sent first into the soft and then into the hard line, the signal strengths shifted accordingly. The LIONs and fibres responded similarly at this low rate, but the LIONs were somewhat noisier.

Dark Current and Field Emission

Losses of dark current emitted by the CW electron gun exceed photocurrent losses through the first short linac (L0B) and the first collimation region (COL0). Also, since dark current and photocurrent gain the same energy, some dark current travels the length of the accelerator and produces losses far downstream. LBLMs integrate both loss sources to provide overall protection.

Field emission from a cryomodule cavity is another loss source unrelated to photocurrent from the gun. In Fig. 2, the A and B fibres spanning the second half of L3B detected a sudden increase in loss that followed the RF amplitude of cryomodule 35 cavity 4 (CM35-4). Losses disappeared when this cavity was shut off. There was also some sensitivity to CM34-7. The observations suggest that electrons emitted at a site in CM35-4 accelerated upstream (the direction depends on the site and emission phase) into CM34, where they were lost. Indeed, a subsequent radiation survey found a hot spot at CM34. The fibre detected this loss signal through the thick cryomodule wall.

ISBN: 978-3-95450-236-3 ISSN: 2673-5350 doi:10.18429/JACoW-IBIC2023-TUP005

Diagnostic Waveforms

The 500-ms *RC* integrator sends the low-frequency component of the PMT signal through an op amp to BCS and MPS. The high frequencies, after a buffer and an external amplifier with adjustable gain, provide a fast diagnostic waveform showing the arrival time of a Cherenkov loss pulse at the PMT. The z coordinate of this loss can be found using a known loss point and the propagation speed (1.5 c).

A wire scanner passing through the beam adds loss peaks downstream. Shot-by-shot numerical integration over these peaks gives the charge scattered by the wire. This is acquired synchronously with the encoder for the wire position to measure beam profiles.

A graphical user interface (GUI) using the Python Display Manager shows the diagnostic waveform, to aid in localizing losses and in setting the integration gate for wire scans. The GUI can plot the waveform of the selected LBLM against time or z, adjust the amplifier's gain, zoom in on a region of interest in the million-point record, highlight the gate interval, and add crosshairs to mark features. The user can pause the running display and, with a buffer of the ten most recent waveforms, toggle back in time, save the buffer, or load a previously saved buffer.

Problems

Commissioning has uncovered various problems.

Gain The gains of all PMTs are set to deliver equal response. Small adjustments of each bias voltage balance the tube-to-tube variation in gain and compensate for the distance to the different fibre locations. We performed initial calibrations (discussed below) to check the attenuation in the thick steel housing of cryomodules for the associated fibres. Conversely, because the 2-km bypass beamline over the NC linacs (FACET-II and LCLS) has a thin stainless-steel beampipe and few magnets to attenuate showers, fibre signals there were quite strong and could saturate the digitiser. We then changed the selectable gain of the op amp following the integrator, raising the gain for cryomodule fibres from 6 to 69 and lowering the gain for the bypass from 6 to 1. In regions that require a low radiation limit—the LTU (in a ground-level bunker) and the Undulator Hall—the gains are set to 20 rather than 6. Calibrations now show that the sensitivities are well balanced.

PMT Failures Since fibre attenuation, both inherent and radiation-induced, increases inversely with wavelength, the LBLMs use red-sensitive cooled PMTs, the Hamamatsu H7422P-40 [1]. These have sensitive GaAsP photocathodes and a low limit of 2 μA on the time-average anode current. Their delicacy may be responsible for a few premature failures that do not appear to be related to this current limit. We have asked Hamamatsu to investigate the failures. This model has since been replaced by the H16722P-40. It may be more robust, with a limit of 40 μA and somewhat higher gain. We have ordered several.

Self-Check The upstream end of each fibre has an LED used for a continuous self-check. Very weak light from the LED is modulated at 0.8 Hz (75 periods of the 60-Hz power line). A lock-in amplifier implemented in a digital signal processor (DSP) selectively detects this frequency in the PMT signal [1]. We have encountered two problems.

A built-in Peltier cooler lets the PMT operate at 0°C, but only if the exterior of the module remains below 35°C. On a hot summer afternoon, the interior of our racks routinely reaches 45 to 50°C. We added a secondary Peltier cooler to our LBLM chassis that limits the PMT housing to 30°C. However, we did not consider that LED emission decreases with temperature, following $\exp(-K\Delta T)$ [4] for a rise ΔT. The coefficient K is 0.00952/°C for the GaP and InAlGaP diodes we use for our different self-check wavelengths [5]. Emission drops by 68% over a temperature range from 10 to 50°C. This shows up as both a diurnal and seasonal variation in the detected self-check amplitude. We are now investigating compensation using a resistor with a negative temperature coefficient in the constant-current loop driving the LED. The emission drop may be reduced to 7%.

Also, sharp spikes in beam loss cause bipolar jumps in the detected self-check. Calculations show that the wide bandwidth of a loss spike passes a jump decaying with the filter's slow (~1 minute) time constant. Superposed on the peak are oscillations at 0.8 Hz damping with the *RC* time constant. A longer digital filter should reduce the effect.

POINT BEAM-LOSS MONITORS

Integrated Loss Signals

PBLMs use a 4-mm-square chip of single-crystal diamond that is 0.5 mm thick (Cividec type B1HV). A beam-loss shower passing through the chip creates electron-hole pairs that are drawn to electrodes plated on opposite faces and biased with a 250-V difference [1]. We have found that only single crystals bring the signal immediately to zero when losses stop [1]. Charge is trapped at the crystal boundaries of polycrystalline material, significantly delaying both the rise and especially the fall of the signal.

Like the LBLMs, PBLM electronics integrate signals with a 500-ms *RC* time constant. Again, MPS should trip first, and BCS only at a higher threshold. Many of the PBLMs for both BCS and MPS hang from the ceiling midway between beamlines of the LTU, to protect both, and cover a region extending about 20 m upstream.

Other PBLMs are mounted at halo collimators and trip only MPS. At this stage of commissioning, scraping in collimators provides most of our PBLM data. In Fig. 3, the $+y$ (vertical) jaw of an LTU collimator was fully open while the $-y$ jaw was scanned across the beam. The charge gradually dropped at the next beam-position monitor (BPM) downstream. The PBLM signal rose as the charge fell.

Figure 4 shows a collimator 2.2 km from the gun, after a dogleg. The photocurrent beam was off, but dark current from the gun reached this spot and heated the collimator jaws, which had insufficient cooling. Shortly before the temperature rise, the PBLM signal jumped up, reaching the saturation level of the digitiser (650 mV). One jaw was opened, and a solenoid at the gun was then refocused to reduce the dark current downstream. The PBLM signal fell abruptly, and the temperature began decreasing.

ISBN: 978-3-95450-236-3 ISSN: 2673-5350 doi:10.18429/JACoW-IBIC2023-TUP005

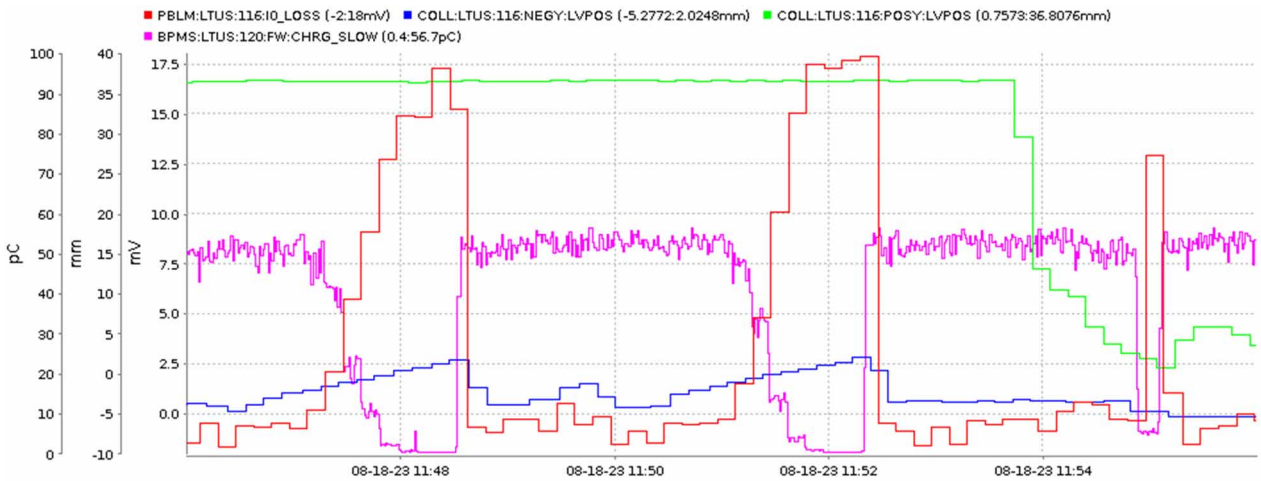

Figure 3: The positive (+y, green) jaw of an LTU vertical collimator was fully open as the negative (−y, blue) jaw scanned across the beam. The bunch charge (magenta) transmitted to the next BPM dropped as the PBLM signal (red) rose.

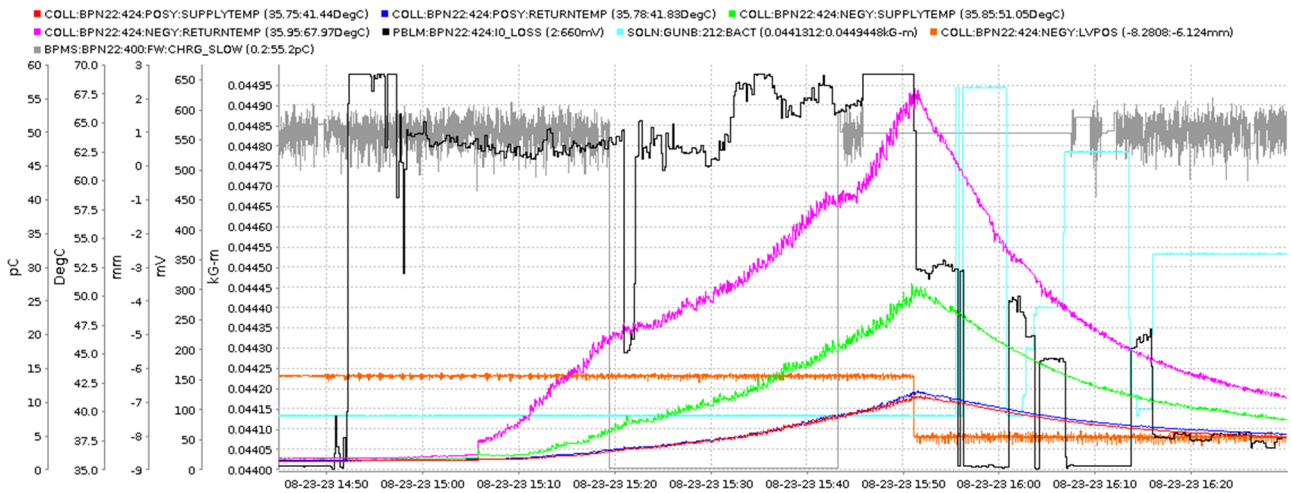

Figure 4: The PBLM signal (black) at a collimator 2.2 km from the gun rose abruptly. Jaw temperatures climbed soon after and continued rising with the photocurrent (grey) off. The loss signal was lowered first by opening the −y jaw (orange) by 1.8 mm and then by lowering dark current with a solenoid at the gun (cyan). The temperatures began to drop.

CALIBRATION

Relating lost beam energy to loss signals is complex, due to the interplay of local shielding, varied beam direction, radiation distribution, and loss location along the accelerator. We get the signal distribution by varying each steering magnet over its full range, one at a time, to cover every beam-loss location and trajectory. To avoid damage, bunches are fired not at a continuous rate but in short bursts of 1 to 100, separated by up to 2 ms. The longer bursts are needed at the low-energy end of the linac to lose enough beam energy. The burst energy is kept well below any known damage thresholds for instantaneous heating. Only one burst per beam-loss trajectory is needed.

We define the sensitivity of a BLM as ratio of the strongest signal (mV) to the lost beam energy (J). The signal-size histogram helps set thresholds, based on the fraction of events we wish to trip on and the energy-loss limit for each region. A setting near full sensitivity would fail to trip on significant loss events, but a low choice would trip frequently on noise.

REFERENCES

[1] A.S. Fisher *et al.*, "Beam-loss detection for the high-rate superconducting upgrade to the SLAC Linac Coherent Light Source", *Phys. Rev. Accelerators and Beams,* vol. 23, p. 082802, 2020. doi: 10.1103/PhysRevAccelBeams.23.082802

[2] A. S. Fisher *et al.*, "Commissioning Beam-Loss Monitors for the Superconducting Upgrade to LCLS", in *Proc. IBIC'22*, Kraków, Poland, Sep. 2022, pp. 207-210. doi:10.18429/JACoW-IBIC2022-TU2C3

[3] J.A. Mock *et al.*, "Commissioning of the LCLS-II Machine-Protection System for MHz CW beams", presented at IBIC 2023, Saskatoon, SK, Canada, Sep. 2023, paper TU3I01.

[4] S.C. Bera *et al.*, "Temperature Behaviour and Compensation of Light-Emitting Diode", IEEE Photonics Tech. Lett. vol. 17, pp. 2286-2288, 2005. doi: 10.1109/LPT.2005.858154

[5] https://tachyonlight.com/analysis-of-the-influence-of-temperature-on-led